

Modelling and Statistical Model Checking of a Microgrid ^{*}

Souymodip Chakraborty Joost-Pieter Katoen Falak Sher^{**}
Martin Strelec^{***}

RWTH University Lehrstuhl für Informatik 2, 52056 Aachen, Germany

Received: date / Revised version: date

Abstract. This paper reports on the modelling and analysis of a microgrid with wind, microturbines, and the main grid as generation resources. The microgrid is modelled as a parallel composition of various stochastic hybrid automata. Extensive simulation runs of the behaviour of the main individual microgrid components give insight into the complex dynamics of the system and provide useful information to determine adequate parameter settings. The analysis of the microgrid focuses on checking linear temporal logic properties, expressed in the logic LTL, using the statistical model checker UPPAAL-SMC.

1 Introduction

Energy is of paramount importance for society. The importance of alternative renewable energy sources like solar and wind is rapidly increasing. The exploitation of these different energy sources leads to a decentralization of the energy production. This development, combined with an increasing resilience on faults and difficulties to upgrade the transmission infrastructure, have resulted in the development of local autonomous energy grids – (smart) *microgrids* [15]. A microgrid can be seen as a localized group of generation, storage and load units that operates with more or less support from the maingrid by buying/selling electricity from/to it when needed.

A microgrid is an independent unit autonomously regulating the energy demands. It may have renewable energy sources, e.g., wind turbines, microturbines, as

well as conventional energy sources such as diesel generators. The main distribution grid remains its major source of electricity. The main power consumers in a microgrid are either household devices or independent units that serve a specific purpose like heating, ventilation or air conditioning (HVAC) units serving one or more buildings collectively. Apart from regulating the production and consumption of energy, a microgrid may also store electricity using batteries, water tanks, etc..

An important objective of a microgrid – in particular when acting in islander mode – is to maintain a balance between producing and consuming energy. Therefore, its supply of energy should not only be stable, safe, and reliable, but also in proportion to its demand. There are many ways to ensure this balance with varying levels of associated cost. The optimal working of a microgrid establishes the supply-demand balance at a minimal possible cost. This raises the question of determining parameters/conditions that ensure power stability in a microgrid at minimal cost. This issue can be settled by a rigorous analysis of a mathematical model of a microgrid.

What kind of model for a microgrid is the most adequate? A microgrid is a real-world system exhibiting continuous behaviour (e.g., electricity is continuously maintained in a grid even at varying levels of consumption) as well as discrete controls (e.g., a local diesel generator can be on or off depending on the electricity demand). Moreover, microgrid behaviour is subject to uncertainties; e.g., a broadcast of an unexpected incident of national importance may result in more TV sets switched on, leading to an increasing demand of electricity. Therefore, we need a modelling formalism that captures probabilistic state changes based on continuously varying quantities – *stochastic hybrid automata* [6]. In the literature, *distributed probabilistic-control hybrid automata* have also been studied for the modeling and analysis of smart grids [22].

^{*} This work has been financially supported by the MoVeS (Modelling, verification and control of complex systems: From foundations to power network applications) EU FP7 project SENSATION and the EU FP7 IRSES project MEALS.

^{**} RWTH Aachen University, Germany

^{***} University of West Bohemia, NTIS, Pilsen, Czech Republic

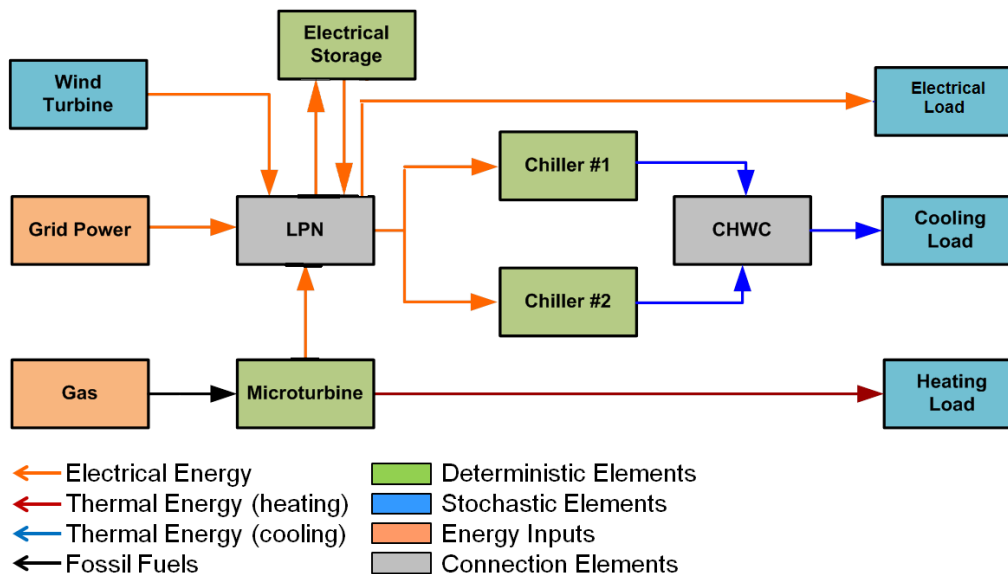


Fig. 1. Configuration of the microgrid case study

Stochastic hybrid automata (SHA) are modeling formalisms in which state spaces are divided into discrete, also called modes of a system, and continuous parts. The behaviour of each mode is given by an ordinary differential equations; and a system can stay in a mode until certain conditions are satisfied. The mode switches are controlled by guards and the next mode (state) of a system is determined by a continuous distribution function over the state space. For details about SHA, we refer to [10].

This paper considers the microgrid configuration depicted in Fig. 15; it extends the configuration in [22] with thermal energy such as the chillers. This microgrid is connected to the electricity and natural gas distribution grids and incorporates two local energy sources – a wind turbine and a microturbine. The microturbine represents a deterministic energy source which produces electricity and heat. The heat can be utilized for satisfying the heating demand such as domestic hot water. The wind turbine is of stochastic nature and its power output depends on actual wind properties. The local power network (LPN) stands for the junction point where the electricity supply meets the electricity demand e.g. chillers, electrical load, etc. Chillers remove the heat from the chilled water circuit (CHWC) which supplies the cooling load with the chill. The demand of cooling load as well as the performances of chillers can be affected by the outside temperature. Electrical energy storage is connected to the LPN and enables the possibility to store/load electricity energy. This can be very useful for the optimization of operational costs of the microgrid.

We model this system as a *composition of stochastic hybrid automata*, and describe their continuous dynamics. For several components of the microgrid we have adopted the dynamics from the literature [9, 19, 23]. Given

the diversity of the continuous phenomena and the strong intertwining with discrete mode switching, we believe that the system model in this paper can act as a benchmark case study for analysis techniques of stochastic hybrid systems. Extensive simulation runs of the behaviour of the microgrid components give insight into the complex dynamics of the system and provide useful information to determine adequate parameter settings. The parameter settings used in our verification models have been obtained in this way and have been validated by Honeywell. For some of the major parameters we show their influence on the analysis results. For the analysis of the microgrid, we resort to *model checking*. Recent developments in model checking of stochastic hybrid systems show the possibility to check a rich variety of properties such as probabilistic reachability and invariance [1], LTL [2]. As the stochastic dynamics and complexity of the microgrid configuration go beyond the scope and feasibility of the above techniques that typically rely on discretization and dynamic programming, we resort here to *statistical* model checking [25, 4]. This technique is basically employing Monte Carlo simulation in order to check the validity of temporal logic properties within a given a priori-defined confidence interval. In order to analyse probabilistic reachability and invariance properties of the microgrid case study, we use UPPAAL-SMC, a recent extension to the model checker Uppaal (www.uppaal.org). UPPAAL-SMC originally focused on (priced and probabilistic) timed automata; however, recently it also covers networks of stochastic hybrid automata [7]. We report on the statistical model checking of several (bounded) LTL formulas and investigate the run-times for various confidence intervals and time horizons. Microgrids have so far received scant attention in the formal modelling and verification community. In

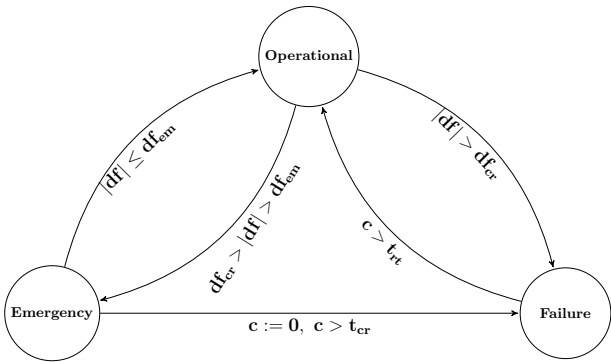


Fig. 2. SHA model of the LPN.

order to analyse microgrid stability, dependability and fairness, in [11], stochastic timed automata (STA) are used as formal models to investigate runtime control algorithms for photovoltaic microgenerators; and in [12] different strategies have been analysed in order to reduce frequency oscillations in a grid. Similarly, in [8] the requirement of the information system of the smart grid is discussed. This system deals with the huge amount of data collected from different parts of the grid in order to maintain its stability.

2 Modelling The Microgrid Configuration

In this section, we explain the model of the microgrid in more detail. We start by discussing the individual components, putting an emphasis on their continuous behaviour. Subsequently, we discuss how the individual models are put together in a compositional manner so as to obtain a model for the entire microgrid configuration. The continuous dynamics of several components is illustrated by some simulation results that were obtained using UPPAAL-SMC.

The **Local Power Network (LPN)** constitutes the junction point that interconnects the main distribution grid, local generators, electrical storage and power loads (see Fig. 1). The power balance equation for the LPN is given by:

$$P_G(t) + P_W(t) + P_M(t) + P_E(t) = \sum_{i=1}^2 P_{Ch,i}(t) + P_D(t) \quad (1)$$

where P_G is the power load from the grid, P_W is the power generated by the wind turbine, P_M stands for the power generated by the microturbine, P_E denotes the power load/supply to/from electrical storage, P_D is the electrical load and $P_{Ch,i}$ is the power demand of the i -th chiller.

The stability of the LPN depends on the balance between power supply (left-hand side of Eq. (1)) and power demand (right-hand side of Eq. (1)). The power imbalance $\Delta P(t)$ denotes their difference. The frequency of

the AC current is typically used as the stability criterion and can be considered as a function of power imbalance $f(\Delta P(t))$. For a stable operation of the microgrid, the frequency may vary only within a certain a priori-defined interval ($[-df_{em}, df_{em}]$) else it goes to emergency mode for a specified amount of time ($[0, t_{cr}]$). Large power imbalances may result in black-outs (if the frequency deviation exceeds df_{cr} or more than t_{cr} time is spent in emergency mode). In the case of a failure, the system is usually restored to operational within t_{rt} . In this configuration, we assume the microgrid is connected to the distribution electricity grid which has the capability to eliminate all imbalances in the microgrid, i.e., $\Delta P(t) = 0$. However, if the microgrid is disconnected from the distribution grid (the so-called islander mode), the stability of the LPN becomes important. The LPN can operate in three discrete modes: *Operational*, *Emergency* and *Failure*. Its discrete dynamics is driven by the frequency deviation df^1 and is naturally captured by hybrid automata (see Fig. 2).

For simplification, we assume that whenever the local production exceeds the consumption, the storage devices are charged. If the grid is operating in islander mode, the discrepancy between production and consumption is balanced by storage P_E as long as it is not drained out. As justified in [3], we do not consider inertia as grid dynamics occur at a much smaller time scale than the phenomena studied here, such as temperature development in rooms and microturbines.

The **wind turbine** is often modelled by a non-linear equation known from the literature e.g., see [16]:

$$P_W(t) = \frac{\pi}{2} \cdot \rho \cdot R^2 \cdot u(t)^3 \cdot C_p(\eta, \theta) \quad (2)$$

where ρ is the air density, R is the blade radius, $u(t)$ is the wind speed, and C_p is an efficiency function depending on θ (the pitch angle) and $\eta = \frac{\omega R}{u}$ is the tip speed ratio, where ω is the rotor speed. (Both θ and η depend on t .) In our studies, however, we utilize wind turbine model based on polynomial approximation of power curve [5] for capturing of wind turbine power production.

$$P_W(t) = a_W u^3(t) + a'_W u^2(t) + a''_W u(t)$$

where a_W, a'_W, a''_W are coefficients. Use of polynomial approximation has two practical reasons (i) power curve can be obtained from manufacturers datasheets, (ii) power curve can be directly identified from common measured data.

A hybrid automaton for the wind turbine has been introduced in [24] and incorporates three discrete modes:

- *Off* - No power is generated by the turbine, e.g., when the wind speed is insufficient to drive the blades.

¹ Frequency deviation stands for deviation of actual frequency from nominal frequency and can be modelled by $df = K_f \cdot \Delta P$ where K_f is a multiplicative constant.

Symbols	constant	values
k_{out}	outside temperature coefficient	0.25 W/K
k_{cw}	chilled thermal coefficient	2250 W/K
C_{CW}	chilled water heat capacity	162280 KJ/W
C_{ZA}	zone air heat capacity	6093 KJ/W
$gain$	average rate of heat gain	75
kv	viscous friction coefficient	0.000011 Nm.s
T	wind speed turbulence factor	1600
κ	geographical location constant	0.00004
$a_{1,i}, a_{2,i}, a_{3,i}$	constants of chiller $i = 1, 2$	0.005,22.22,9.53 0.021,22.22,3.17
$a_{1,OA}, a_{2,OA}, a_{3,OA}$	outside temperature parameters	0.05,0.001,0.2
$a_{0,M}, a_{1,M}, a_{2,M}$	electric torque constants (start)	-0.002,0.15,0
$a_{3,M}, a_{4,M}, a_{5,M}, a_{6,M}$	mechanical torque constants	167.906,132.348 -24.371,0
$a_{10,M}, a_{11,M}, a_{12,M}$	microturbine power curve constants	7.100,-0.0005 0.0000007
m_f^{min}	minimum fuel flow	0.15
$k_{m_f,P}, k_{m_f,I}$	PI controller const. of MT fuel flow	3,1
$k_{P_M,P}, k_{P_M,I}$	PI controller const. of MT power	50,5
$k_{CW,P}, k_{CW,I}$	PI controller const. of chilled water temperature	0.5
$k_{X_c,P}, k_{X_c,I}$	PI controller const. of thermostat	3,1

Table 1: Microgrid constants

- *Power optimization* - Power is generated by wind speed according to polynomial approximation of the Eq. (2).
- *Power limitation* - The turbine reached its maximum production capability $P_{W,max}$.

The wind turbine is considered as a deterministic system given by Eq. (2), which is affected by stochastic inputs. These inputs depend on the pitch angle θ and the wind speed u . There are several modelling approaches in the literature encompassing these two inputs. For example, modelling of wind variability via discrete Markov chains is described in [18]. Alternative approaches are based on time-series models [20]. We assume an optimal placement of the wind turbine against the wind direction θ . Therefore, the power of the wind turbine only depends on the wind speed u . We adopt a one-dimensional stochastic differential equation to model this:

$$du(t) = -\frac{u(t) - \bar{u}(t)}{T} \cdot dt + \kappa \cdot \bar{u}(t) \cdot \sqrt{2/T} \cdot dW(t) \quad (3)$$

where \bar{u} denotes hourly averages of wind speed, κ is a constant depending on the geographical location of the wind turbine, dW is a Wiener process that models the uncertainty in the actual and the forecasted wind speed, and $T = L/\bar{u}$, where L is the turbulence length scale. Fig. 3 and 4 depict two simulations for the wind speed and the corresponding power P_W generated by the wind turbine. The similarity between the plots is apparent as high wind speed results in high power generation.

The *microturbine* influences the electrical and thermal power dynamics of the microgrid. The operation of

a microturbine can be divided into eight separate discrete modes [23]. Mode transitions are guarded by the turbine angular velocity ω whose evolution is defined as:

$$J \cdot \dot{\omega} = T_M(t) + T_E(t) - F_V(t) ,$$

where J is the moment of inertia of the turbine, T_E refers to the electrical torque, T_M is the mechanical torque, and F_V is the viscous friction defined by $F_V(t) = k_V \cdot \omega(t)$.

The discrete modes are:

- *Off* – Device is turned off.
- *Start up* – Turbine accelerates to 25000 rpm (ω_{start}). In this mode, the turbine generator acts as motor and consumes electrical power. The electrical power P_M is the driving force of the turbine (T_E is positive and P_M is negative) and yields:

$$T_E(t) = a_{0,M} + a_{1,M} \cdot P_M(t) + a_{2,M} \cdot P_M(t)^2.$$

The power requirement is modelled by a feedback loop in order to reach the desired angular velocity of ω_{start} in the following way:

$$P_M(t) = k_{P_M,P} \cdot (\omega_{start} - \omega(t)) + k_{P_M,I} \cdot \int_0^t (\omega_{start} - \omega(\tau)) \cdot d\tau.$$

In the literature (e.g. [23]), different feedback controllers are applied for microturbine speed control (e.g. PID), however, we consider PI controller with non-oscillating behaviour for sake of simplicity. Derivative part can be easily incorporated into the model and consequently controllers' constants can be properly designed, but this is out of scope of this article.

- *Stabilization* – Short period before gas ignition where the angular speed of the turbine is constant $\omega = 25000$ rpm.

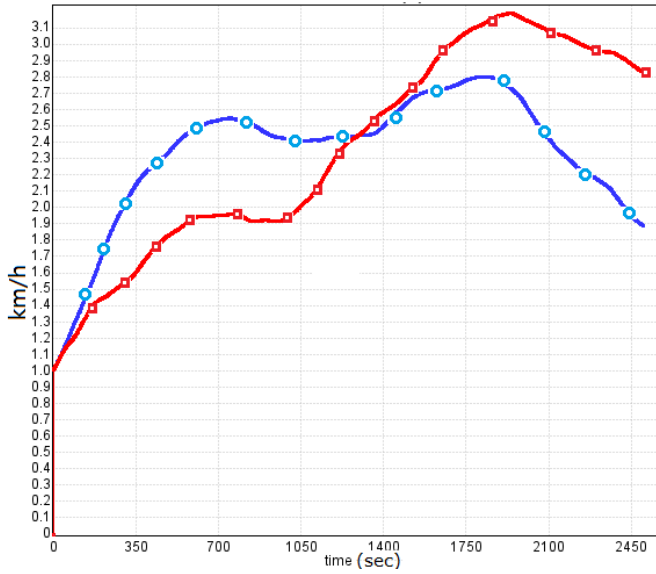


Fig. 3. Simulation of wind speed $u(t)$. In both simulations $k = 0.00004$, $\bar{u}(t) = 2\text{km/h}$, $T = 1600\text{s}$

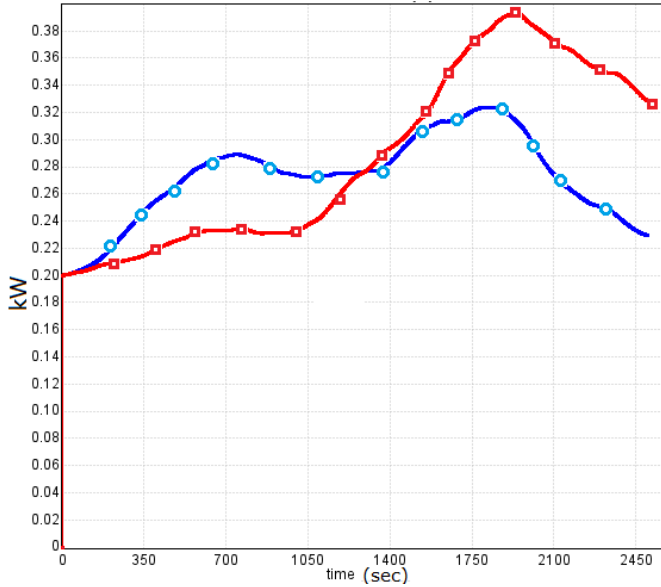


Fig. 4. Generated wind turbine power P_W . Same parameters as Fig.3.

- *Acceleration* – Electrical torque from the generator drives the turbine speed to 45000 rpm. At the end of the interval, it comes to the ignition. The minimal fuel flow maintains the combustion process but does not produce mechanical torque. Torque T_M is zero.
- *Warm up* – The microturbine consumes only fuel, whence $P_M = 0$. The energy from the combustion keeps the turbine at the desired speed of 45000 rpm. T_M provides the necessary mechanical torque, see Fig. 4. The fuel flow and angular velocity oscillate before attaining equilibrium (modeled by PI control equation 4).
- *Operational* – The microturbine produces power and the turbine is driven of the fuel combustion. T_M is

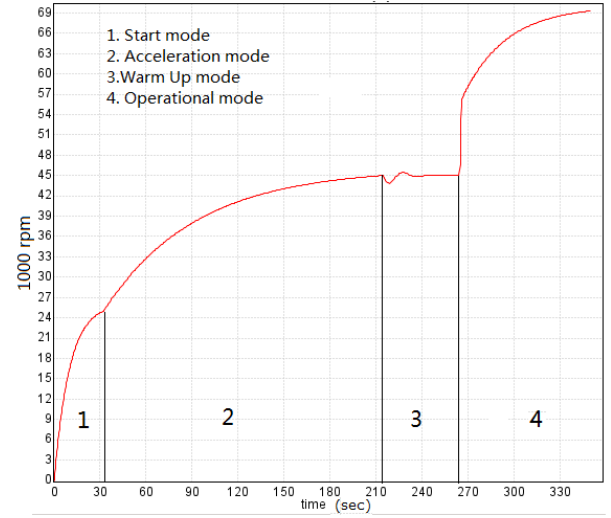


Fig. 5. Turbine angular velocity ω

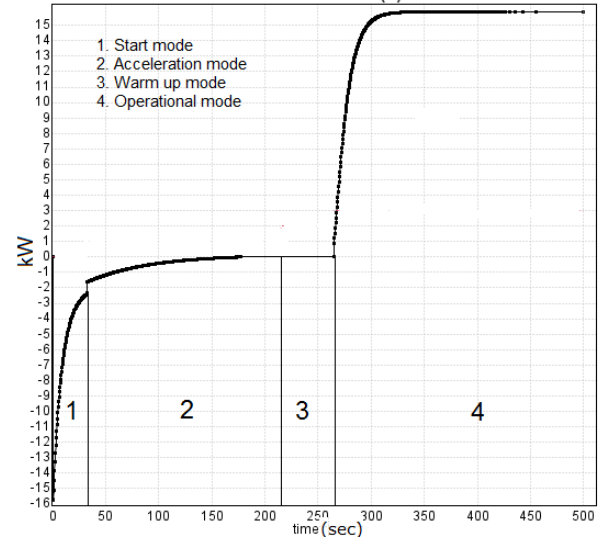


Fig. 6. Microturbine power P_M

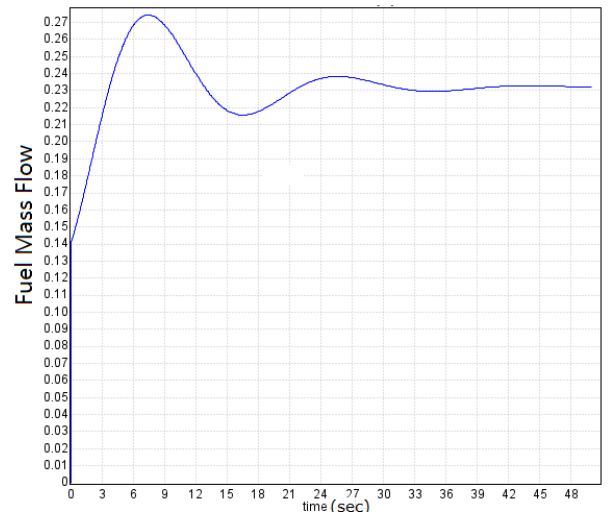


Fig. 7. Fuel mass flow during warm up m_f

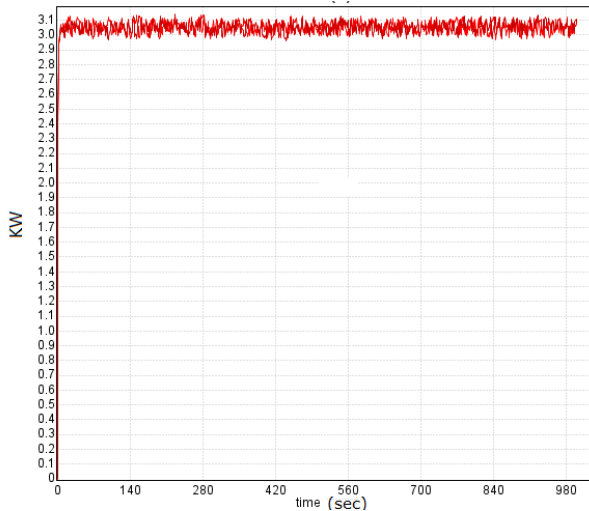


Fig. 8. Electric load in the microgrid P_D

the driving force for the rotation of turbine. Electrical power is generated (P_M is positive) and the emerged electromagnetic field tends to slow down the turbine rotation hence (T_E is negative):

$$\begin{aligned} T_M(t) &= a_{3,M} + a_{4,M} \cdot m_f(t) + a_{5,M} \cdot m_f(t)^2 - a_{6,M} \cdot \omega(t), \\ T_E(t) &= a_{7,M} + a_{8,M} \cdot \omega(t) + a_{9,M} \cdot \omega(t)^2, \\ P_M(t) &= a_{10,M} + a_{11,M} \cdot \omega(t) + a_{12,M} \cdot \omega(t)^2. \end{aligned}$$

The power at which the microturbine should eventually operate determines the desired speed (ω_{SP}) of the turbine. The fuel flow m_f is controlled by a PI controller to keep the turbine at a ω_{SP} according to:

$$\begin{aligned} flow(t) &= k_{m_f,P} \cdot (\omega_{SP} - \omega(t)) + \\ &\quad k_{m_f,I} \cdot \int_0^t (\omega_{SP} - \omega(\tau)) d\tau, \\ m_f(t) &= \min\{m_f^{min}, flow(t)\}. \end{aligned} \quad (4)$$

- *Slow down* – The generator is disconnected from the LPN and the turbine is slowed down to $\omega = 25000$ rpm.
- *Cool down* – Fuel supply is closed ($m_f = 0$). Microturbine slows to stop ($\omega = 0$).

The heat produced from the combustion of fuel serves the heating load (e.g., domestic hot water) by:

$$Q_M(t) = a_{13,M} + a_{14,M} \cdot m_f(t) + a_{15,M} \cdot m_f(t)^2.$$

Fig. 5 shows the angular velocity of the turbine from start to operational mode. Fig. 6 shows the power characteristics of the microturbine where the value P_M is negative from start to acceleration mode. Only during the operational mode (when the microturbine produces energy), P_M is positive. Fuel injection starts in the acceleration mode. This component is not stochastic.

Electrical storage is the device that enables storing electrical energy over time. We use the storage model

of [19] where the electrical storage evolves according to the following differential equation:

$$\frac{dP_S}{dt} = -\gamma \cdot P_E(t) - P_L(t), \quad (5)$$

where P_S expresses the stored energy level in the storage, γ denotes the power exchange efficiency, P_E is the power exchanged between the storage and the LPN, and P_L stands for power losses associated to the storage. Electrical storage can operate in five discrete modes:

- *Supply* - The device drains energy $P_E > 0$ with efficiency $\gamma = \gamma_s$.
- *Store* - No exchange of electricity $P_E = 0$; electrical energy leaks at rate P_L .
- *Load* - The device acts as a load $P_E < 0$ and recharges its energy level with efficiency $\gamma = \gamma_l$.
- *Full* - Storage reaches its maximum capacity $P_{ES} = P_{ES,max}$.
- *Drained* - Stored energy level is on the minimal capacity $P_{ES} = P_{ES,min}$.

P_E denotes an input variable quantifying the power supplied (loaded) from (over) the storage device in connection with the LPN. We consider P_E as the difference between the local power production and load.

Chiller is an electrical device that converts electrical energy into thermal energy (cooling energy). We use the Gordon-Nq model of the chiller [9], where the power demand P_{Ch_i} of chiller i ($i = 1, 2$) is given by:

$$P_{Ch_i} = \frac{a_{3i} Q_{cool,i}^2 + (Q_{cool,i} + a_{2i})(T_{OA} - T_{CW}) + a_{1i} T_{OA}}{T_{CW} - a_{3i} Q_{cool,i}}$$

where $Q_{cool,i}(t)$ is the thermal energy removed by the i -th chiller at time t . The power demand of a chiller evolves continuously because of its dependency on other continuous quantities such as outside temperature. $Q_{cool,i}$ thus represents the (portion of the total cooling Q_{cool}) energy required by the system from chiller i . Its value is decided based on a selected control policy. The total energy demand Q_{cool} is modelled by a PI (proportional, integral) controller. Its value depends on two quantities: the chilled water temperature T_{CW} and its desired value (setpoint) $T_{CW,SP}$. Our microgrid model has two chillers. The energy requirement is hence distributed among them. This distribution is controlled by an input parameter $\alpha_{Ch}(t)$, i.e., $Q_{cool,1}(t) = \alpha_{Ch}(t) \cdot Q_{cool}(t)$ and $Q_{cool,2}(t) = (1 - \alpha_{Ch}(t)) \cdot Q_{cool}(t)$.

The **outside temperature** is given by a modified Uhlenbeck-Ornstein stochastic differential equation:

$$dT_{OA} = a_{1,OA} \cdot (T_{OA}^f - T_{OA}(t)) dt + a_{2,OA} \cdot dT_{OA}^f(t) + a_{3,OA} \cdot dW \quad (6)$$

where T_{OA}^f is the forecasted outside temperature, and dW is the Wiener process that models the uncertainty in the actual and the forecasted temperature.

The **cooling load** is modelled by modified lumped thermal model (e.g. [17]) which represents a building consisting of n rooms (zones), denoted Z_i for $i = 1 \dots n$. The

zone temperature T_{ZA} (at time t) evolves according to the stochastic differential equation:

$$C_{ZA} \frac{dT_{ZA}}{dt} = X_C(t) \cdot k_{cw} \cdot (T_{CW}(t) - T_{ZA}(t)) + k_{out} \cdot (T_{OA}(t) - T_{ZA}(t)) + NP(t) \cdot gain$$

where $T_{CW}(t)$ is the temperature of the coolant, $X_{cool}(t)$ the thermostat valve position, C_{ZA} is the thermal capacity of the zone, k_{cw} is a heat transfer coefficient for zone-chilled water, k_{out} is a heat transfer coefficient for zone-outside air and $gain$ stands for the heat produced by one person. The stochastic aspects here are the number of people $NP(t)$ in a zone and the outside air temperature $T_{OA}(t)$ which is given by Eq. (6). It is assumed that each person increases the zone temperature by a constant $gain$ per time interval.

The function of the thermostat is to regulate the temperature of the room T_{ZA} by changing the value of X_C . The thermostat is modelled by a PI controller and the value of X_C depends on two other quantities, the desired temperature of the zone T_{ZASP} and the current zone temperature T_{ZA} , along with proportional $k_{X_C,P}$ and integral $k_{X_C,I}$ constants:

$$\begin{aligned} e(t) &= T_{ZA}(t) - T_{ZASP}(t), \text{ and} \\ temp(t) &= k_{X_C,P} \cdot e(t) + k_{X_C,I} \cdot \int_0^t e(t) dt \quad (7) \\ X_C(t) &= \max\{0, \min\{temp(t), 100\}\}. \end{aligned}$$

Fig. 9 and Fig. 10 show the evolution of the room temperature and thermostat value, respectively when the set-point temperature T_{ZASP} is at 25°C (blue), 22°C (green), and 20°C (red).

The **Chilled Water Circuit (CHWC)** captures the behaviour of the coolant temperature $T_{CW}(t)$ which interacts with zone temperature $T_{ZA}(t)$ and with chillers. The chilled water circuit temperature T_{CW} is modelled by a modified lumped thermal model and evolves according to the following differential equation:

$$C_{CW} \cdot \frac{dT_{CW}}{dt} = X_C(t) \cdot k_{cw} \cdot (T_{ZA}(t) - T_{CW}(t)) - Q_{cool}(t)$$

where C_{CW} is the thermal capacity of the water circuit and Q_{cool} is the thermal energy removed by chillers².

The **chilled water temperature controller** keeps the chilled water temperature at the set point value T_{CWSP} (another control parameter). The energy requirement is controlled by a feedback loop and hence designed as a PI control scheme:

$$\begin{aligned} e_C(t) &= T_{CW}(t) - T_{CWSP}(t), \\ temp(t) &= k_{CW,P} \cdot e_C(t) + k_{CW,I} \cdot \int_0^t e_C(\tau) d\tau, \\ Q_{cool}(t) &= \min\{0, \min\{Q_{max}, temp(t)\}\}, \end{aligned}$$

² $Q_{cool}(t) = Q_{cool,1}(t) + Q_{cool,2}(t)$.

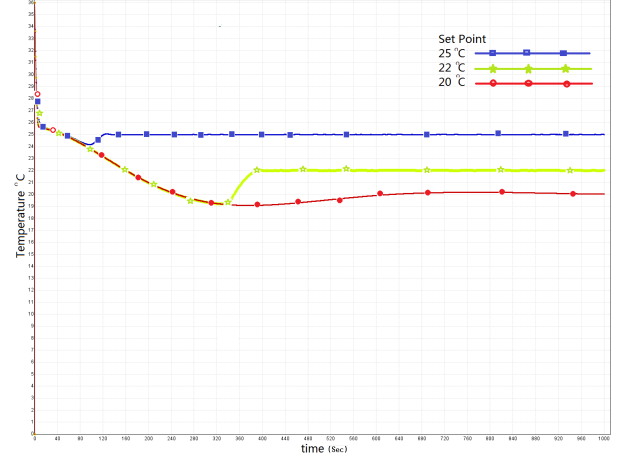


Fig. 9. Room temperature T_{ZA}

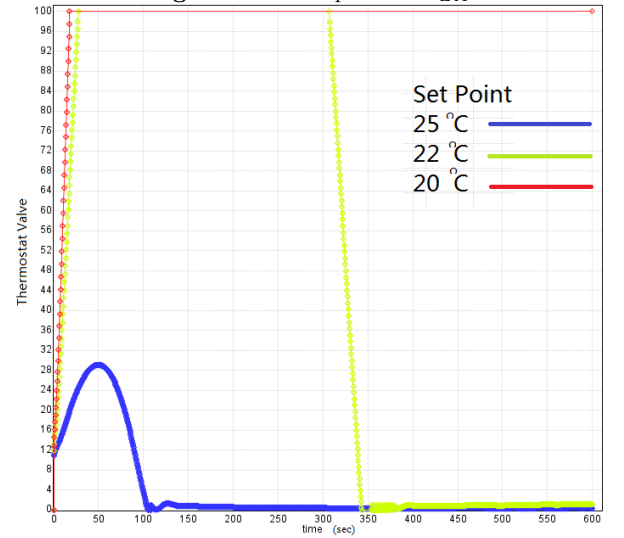


Fig. 10. Thermostat value X_C

where Q_{max} is the maximum energy requirement that can be met by the chillers. Fig. 11 and 12 show the behaviour at set points 20°C, 15°C, and 10°C, respectively.

The **electrical load** is modelled according to Uhlenbeck-Ornstein differential equation which captures its continuous dynamics. It has two modes: *Connected* or *Disconnected*. When connected the stochastic differential equation reads:

$$dP_D = a_{1,D} \cdot (m(t) - P_D(t)) \cdot dt + \sigma_D \cdot dW,$$

where $m(t)$ is a given load profile³, $a_{1,D}$ represents a tracking coefficient, σ_D is a variation coefficient, and dW denotes the Wiener process. In the case of the Disconnected mode, the dynamics of electrical load is trivial as $P_D = 0$, $dP_D/dt = 0$. A simulation is shown in Fig. 8.

³ A load profile captures typical pattern of the load which can be expressed in a form of mean values for given time instances (e.g. daily load pattern).

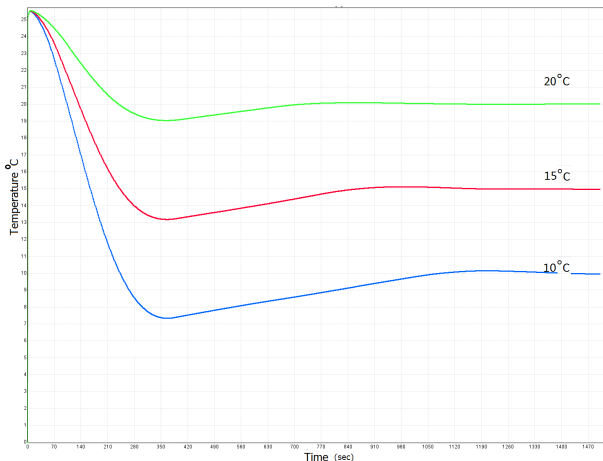


Fig. 11. Coolant temperature T_{CW}

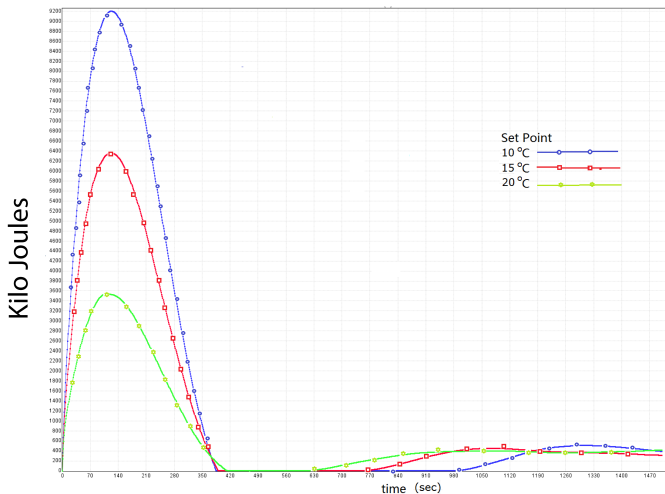


Fig. 12. Energy requirement Q_{cool}

The **heating load** represents a small demand for heating (i.e., domestic hot water) which is supplied by wasted heat from the microturbine. This load depends on occupants activity during the day and can be considered as stochastic process which can be modelled in a similar fashion as the electrical load above⁴.

Overall microgrid model. We have modelled all individual components as stochastic hybrid automata. Let LPN , CH_i , $CHWC$, Z_j , MT , WT , ST , EL be the SHA models of the local power network, the i^{th} chiller, the chilled-water circuit, the j^{th} room (or zone), microturbine, wind turbine, storage, and electrical load, respectively. The composite SHA model of the microgrid is now given as:

$$MG = (LPN \parallel CH_i \parallel CHWC \parallel Z_j \parallel MT \parallel WT \parallel ST \parallel EL)$$

where $i = 1$ to 2 , $j = 1$ to n and \parallel denotes a parallel composition operator (for details about \parallel , we refer to [10]). Note that our composite model is simple in a

sense that there is no synchronization among different components of the grid.

Resolution of non-determinism in composite model. In the network of SHA, each SHA continuously race against each other component, i.e., they independently and stochastically decide about the duration of their stay in a specific mode; and the winner is the one that decides for a minimum duration. In UPPAAL-SMC tool, the components which can stay in a mode indefinitely, decide about the duration of their stay using an exponential distribution; and those who cannot stay more than a specific time period, decide their duration using a uniform distribution.

Controllers and scenarios. There are various input parameters for the different components of the microgrid. Controllers are designed to modify these inputs in order to satisfy some optimality criteria, usually to minimize power consumption. Various controllers can be modelled by automata. The effect of these controllers can be studied by running the respective automaton in parallel with the microgrid. For example, we can consider an automaton that depending on the required cooling power and ambient temperature, distributes the energy among the two chillers accordingly. It is possible that some chillers work better at lower energy requirements than others. In one experiment we modified the control parameter $\alpha_{ch}(t)$ which distribute the cooling energy production between chillers from constant value (static) to a more dynamic one which changes according to the energy requirement. In Fig. 13, we can see the total power consumed by the chillers under the two different type of control parameter α . We know before hand that the chiller 1 performs better at low load than chiller 2. In this experiment we start with initial room temperature of 36° and coolant temperature 25° , we selected a threshold $2000KJ$ above which the distribution of the cooling energy production changes from $(0.8 : 0.2)$ to $(0.5 : 0.5)$.

We are also interested in testing the behaviour of the microgrid under special conditions, e.g., observing the frequency deviation over time when the microgrid is disconnected from the main grid (islander mode). Fig. 14 shows the frequency deviation when the microgrid is running in islander mode with 2 wind turbines and one microturbine providing for two chillers and one electric load along with a storage device. As the microgrid is cut off from the main grid, the power generated by wind turbines is insufficient (in this experiment) and hence the batteries were catering for the power deficit. At the same time the microturbine is powered up. We have seen from the simulation runs of the microturbine, that in the initial phase it draws power. The load of the grid is kept independent of the energy production. The temperature set points for the cooling ($T_{CWSP} = 17^\circ$, $T_{ZASP} = 20^\circ$) and the power distribution for the chillers ($\alpha = (0.6 :$

⁴ I.e. Stochastic process based on Uhlenbeck-Ornstein model.

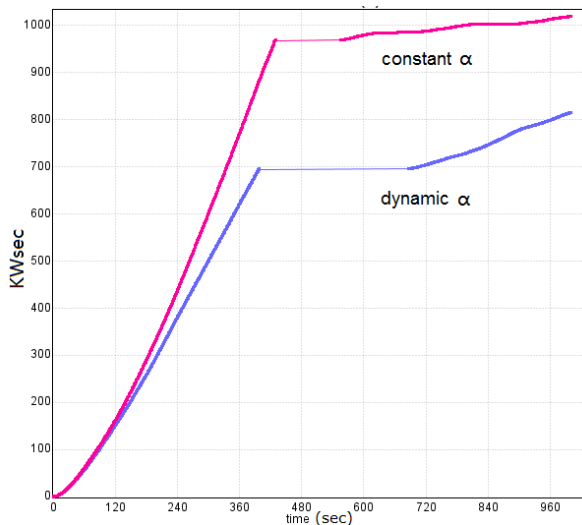


Fig. 13. Cumulative electrical power consumed by the chillers

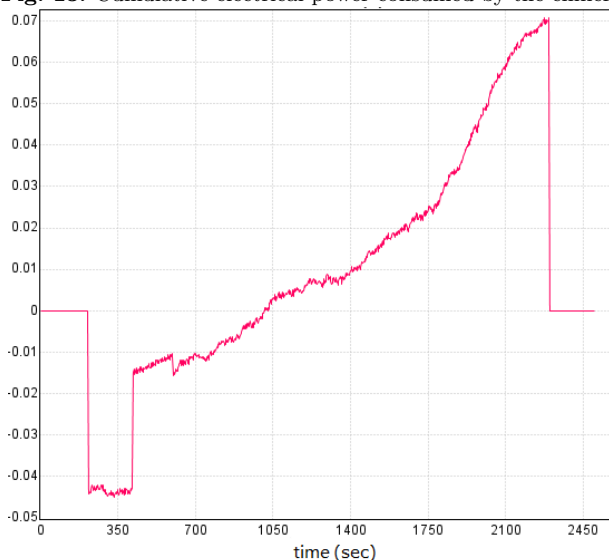


Fig. 14. Frequency deviation

0.4)) are kept constant. Thus, the batteries soon run out and we have observe a negative frequency deviation. When the microturbines is accelerated to operational speed it provide (more than) enough energy for the demand, hence we see a positive deviation. Finally, the batteries start to recharge themselves to use up the excess power and the frequency stabilizes.

3 Model Checking the Microgrid

The properties of a microgrid that we are interested in, are expressed as bounded linear time formulas. For instance, how likely is it that the temperature of various cooling devices reach a required set of values, or the energy requirement exceed some threshold with a given outside behaviour, or a microgrid becomes unstable in islander mode, etc.

Numerical methods to solve model-checking problems of stochastic hybrid systems against some temporal formulas (even reachability) are algorithmically involved and suffer from the curse of dimensionality [1, 2, 21]. Statistical model checking avoids these problems by resorting to discrete-event simulation (using Monte-Carlo techniques). In a nutshell, it generates and examines finitely many simulation runs of a model at hand, and uses hypothesis testing to infer whether the obtained simulation samples provide statistical evidence for the satisfaction or violation of some (temporal logic) specification [25, 4].

Statistical model checking in a nutshell. We briefly describe the main principles of statistical model checking and refer to [26] for a more detailed explanation. Let X be a stochastic process, which could be as simple as a Markov chain or as complex as a closed (i.e., needs no external decision) stochastic hybrid automaton. Let φ be a property defined by some temporal bounded logic, say bounded LTL. A finite trajectory ρ of X , also called an execution, satisfies (denoted \models) the property φ if and only if the trace of ρ belongs to the language of φ . The problem is to decide whether:

$$P : \Pr[X \models \varphi] \geq \theta,$$

holds for $\theta \in [0, 1]$. This is accomplished by inspecting a limited number of finite executions of X , called *test samples*. Obviously, we want the size of the test sample, denoted n , to be as small as possible such that the probability of making an error is small. One can observe that for bounded reachability properties it is possible to figure out traces in a test sample that are words of φ , which is not the case with unbounded reachability properties.

The aim now is to test the hypothesis $H : \Pr[X \models \varphi] \geq \theta$ against $K : \Pr[X \models \varphi] < \theta$. Let ζ be the probability of accepting K when H holds (false negative) and β the probability of accepting H when K holds (false positive). It is not possible to have n for which both ζ and β are small. Hence, in practice one checks the hypothesis $H_0 : \Pr[X \models \varphi] \geq \theta + \delta$ against $H_1 : \Pr[X \models \varphi] \leq \theta - \delta$, where $\delta (\delta \geq 0)$ is the indifference region. This procedure is indifferent to the decision whether $|\Pr[X \models \varphi] - \theta| < \delta$.

Different ways of finding a test procedure with the above mentioned characteristics exist, e.g., the *fixed size sample method*. Other methods are, for example, the *sequential ratio test method*. For an overview and empirical comparison we refer to [14]. The fixed size sample method briefly works as follows. A sample of size n contains the observations ρ_1, \dots, ρ_n , with the associated random variable x_1, \dots, x_n (i.e., $x_j = 1$ iff $\rho_j \models \varphi$). To test hypothesis H_0 against H_1 , we specify a quantity c ($c \leq n$). H_0 is accepted if $\sum_{j=1}^n x_j > c$. Observe that the random variables $\{x_i\}_{i \leq n}$ are i.i.d. with $\Pr[x_i = 1] = \Pr[X \models \varphi]$. Let $\Pr[x_i = 1] = p$. The prob-

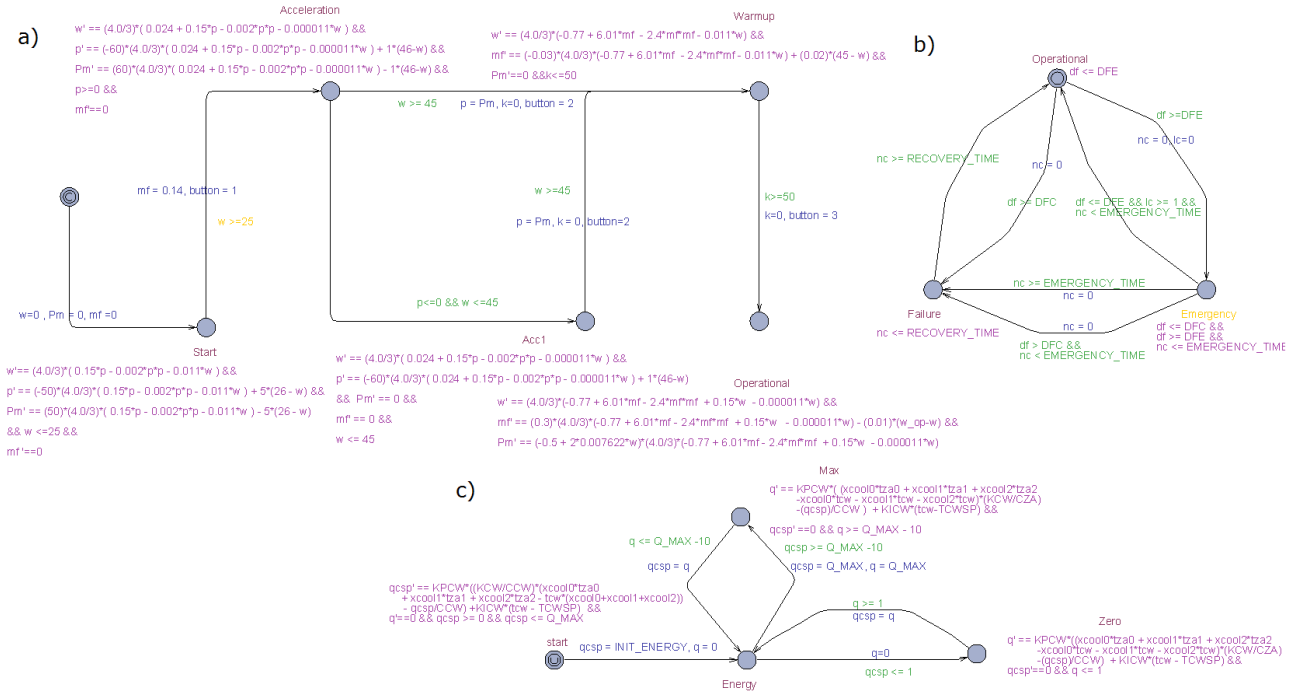


Fig. 15. The figure a) shows the UPPAAL model of the first four stages of microtubine, b) shows the local power network, c) shows the chilled water controller ($qcsp$ is the chiller energy demand Q_{cool}).

ability of $\sum_{j=1}^n x_j$ being at most c is:

$$F(c, n, p) = \sum_{i=0}^c \binom{n}{i} p^i \cdot (1-p)^{n-i}$$

Thus, the problem is to find a pair (n, c) which satisfies $F(c, n, p) \leq \zeta$ when $p \geq \theta + \delta$, and $1 - F(c, n, p) \leq \beta$ when $p \leq \theta - \delta$. Since $F(c, n, p)$ is a non-increasing function in $p \in [0, 1]$, this yields the following (non-linear) optimization problem to minimize n :

$$\begin{aligned} F(c, n, \theta + \delta) &\leq \zeta, \\ 1 - F(c, n, \theta - \delta) &\leq \beta. \end{aligned}$$

This yields us the required n and test criterion c . The details of dealing with nested formulas (see [26]) are not relevant for our case study as all properties of interest are un-nested formula.

The UPPAAL-SMC tool. We analyse microgrid model using the UPPAAL-SMC tool. UPPAAL-SMC focus mainly on networks of priced timed automata. These are timed systems in which real variables may have different rates (even potentially negative) in different modes. These variables are not used as guards. A recent extension of this tool allows to handle stochastic hybrid automata, first reported in [7]. Here, the change of continuous variables is governed by linear differential equations. Euler's method of first order approximation for ordinary differential equations is employed to restrict the change in real variables to constant rates.

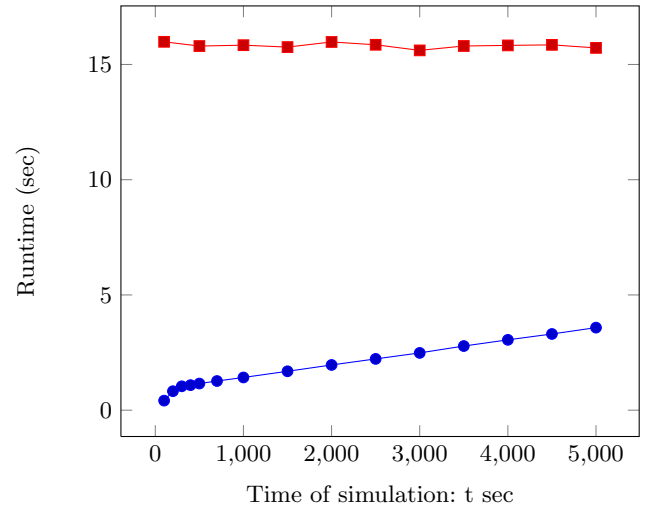


Fig. 16. Simulation (blue ●) and model checking (red ■).

UPPAAL-SMC relies on results from statistics such as sequential hypothesis testing and Monte Carlo simulation. Crucial statistical input parameters are the confidence ξ which quantifies the error, given by the parameter ζ and β (as before), and the probability interval defined by the indifference region δ . Apart from being able to simulate various variables, we can carry out statistical model checking of temporal logic formulas expressed in bounded LTL. For example, we can check whether the likelihood of reaching a specific set T of target states within m time units is greater than p or

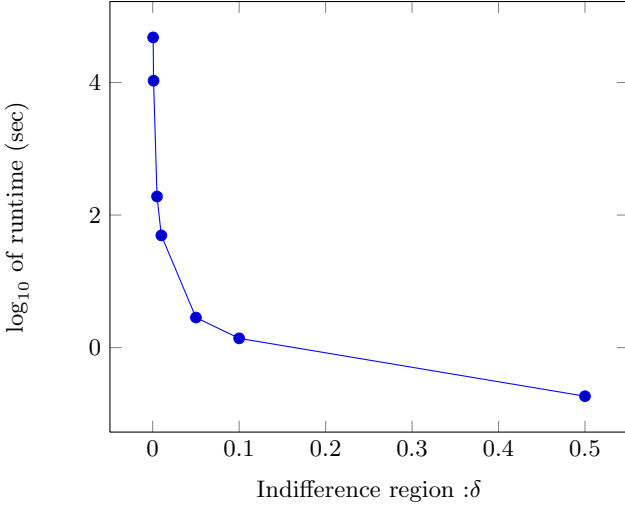


Fig. 17. Indifference region vs runtime.

not ($\Pr(\diamond_{\leq m} T) > p$), or the probability to stay in a given set \bar{T} of states for the next m time units is less than p ($\Pr(\square_{\leq m} T) < p$).

Scalability. Simulation runs of a microgrid depict the dependency of different parameters on each other. For example, the cooling load (CL) of a microgrid — that is dependent on outside ambient temperature, the number of rooms, thermostat values, chilled water circuit and chilled water temperature controller — varies with time as given in Fig. 16 (we assume the number of people entering or leaving the room are binomially distributed.). We see that there is almost a linear relationship between CL and time.

Fig. 16 also presents the runtime of model checking the formula $\varphi = \diamond_{\leq t}(Q_{cool} > 4000\text{kJ})$ with $T_{ZASP} = 20$ and $T_{CWSP} = 17$. Note that increasing the value of t in φ has no significant effect on the runtime of the model checking algorithm. This is because φ is satisfied within 300 sec (Table 2) with high likelihood.

We can also vary different statistical model checking parameters and observe the effect on runtime. For example, number of runs increases very rapidly (at least exponential) when the indifference region δ is decreased. The runtime of model checking formula $\diamond_I(|T_{ZA} - T_{ZASP}| \leq 1)$ with $T_{ZASP} = 20$ and $T_{CWSP} = 17$ on cooling load for varying value of δ is shown in Fig. 17.

Temporal properties. For the microgrid case study we are mainly interested in reachability properties. We do hypothesis testing using UPPAAL-SMC version 4.1.11. The first property of interest is the high likelihood of the room temperature being close to the desired set point within some finite time interval. The initial value of the room and water coolant temperature is 35° and 25° , respectively. We vary the value of the time interval and the temperature set points in order to investigate its impact on the runtime. The hypothesis testing results are

listed in Table 2. The first, second and third column defines the property. The fourth and fifth column indicate the values of the control inputs (temperate set points). The sixth and seventh column indicate the confidence and δ of the SMC algorithm (where confidence = $1 - \zeta$ or $1 - \beta$ and δ is the indifference interval) and the last column presents the runtime of UPPAAL-SMC.

The first property refers to the high likelihood of zone temperature T_{ZA} differing at most one degree Celsius from the desired room temperature T_{ZASP} in a given time interval. The second property checks the high likelihood of the chilled water temperature T_{CW} being close to its set point T_{CWSP} . Both these properties are found to be true (conforming to the simulations). The third property is a conditional property, where we check if the room temperature is close to the set temperature then the thermostat valve is not (fully) open. The last property focuses on the cooling energy Q_{cool} , as realized by a PI controller, reaching a threshold of 400 kJ. Observe how the probability changes from very unlikely to highly likely when we change the internal parameters of the model. The effect is also reflected on the runtime.

As a next property, Table 3, we are interested in the behaviour of the chillers. We have the cooling load (CL) along with two chillers. The parameter we change is the distribution parameter α , T_{CWSP} and T_{ZASP} . The LTL-property of interest is the likelihood that the chiller's power demand (of the first chiller, say) exceeds a certain threshold (1 kWh, say) within interval I .

Table 4 presents the results of checking whether the maximum generated power by the wind turbine exceeds some threshold (Max). Unlike Q_{cool} , P_W shows more random behaviour, so the run is not as predictable as in the case of the cooling load. We apply statistical model-checking to calculate the probabilities (range of the probability) in favour of the hypothesis testing. Note that, relaxing the probability interval has a greater effect on the runtime than changing the confidence. The reason being the number of runs for verification increase sharply by lowering δ (see Fig. 17).

Lastly, we check whether the microgrid is stable or not when it goes into the islander mode. We assume the grid stability is characterized by the frequency deviation. We consider the following components: cooling load (CL), one electrical load (EL), wind (W), wind turbines (WT), storage (ST), microturbine (MT) and the local power network (LPN). We consider various situation where we vary availability of storages devices, number of wind turbine at our disposal and whether microturbine is already in warm-up stage or not. Some verification results are listed in Table 5.

4 Conclusions

In this paper we have presented a model of a microgrid configuration as a composition of stochastic hybrid

LTL formula	$I(\text{sec})$	$\prec p$	T_{ZASP}	T_{CWSP}	Confidence	δ	time (sec)
$\diamond_I(T_{ZA} - T_{ZASP} \leq 1) \prec p$	[0, 200]	≥ 0.98	20	17	0.95	0.05	1.874
	[0, 3000]	≥ 0.98	20	17	0.95	0.05	1.968
	[0, 3000]	≥ 0.98	25	20	0.95	0.05	1.307
	[0, 3000]	≥ 0.98	25	20	0.995	0.005	1.647
	[0, 3000]	≥ 0.998	25	20	0.9995	0.0005	2.011
$\diamond_I(T_{CW} - T_{CWSP} \leq 1)$	[10, 200]	≥ 0.98	20	17	0.95	0.05	16,627
	[10, 3000]	≥ 0.98	20	17	0.95	0.05	16.638
	[10, 3000]	≥ 0.98	25	20	0.95	0.05	16.03
	[10, 3000]	≥ 0.98	25	20	0.995	0.005	28.185
	[10, 3000]	≥ 0.998	25	20	0.9995	0.0005	393.832
$\diamond_I(T_{ZA} - T_{ZASP} \leq 1 \wedge X_c > 5)$	[0, 200]	≥ 0.98	20	17	0.95	0.05	13.085
	[0, 3000]	≥ 0.98	20	17	0.95	0.05	13.069
	[0, 3000]	≥ 0.98	25	20	0.95	0.05	1.787
	[0, 3000]	≥ 0.98	25	20	0.995	0.005	2.48
	[0, 3000]	≥ 0.998	25	20	0.9995	0.0005	25.104
$\diamond_I(Q_{cool} \geq 4000)$	[0, 200]	≥ 0.98	20	17	0.95	0.05	5.08
	[0, 1000]	≥ 0.98	20	17	0.95	0.05	5.162
	[0, 1000]	≤ 0.02	20	15	0.95	0.05	16.048
	[0, 1000]	≤ 0.02	20	15	0.995	0.005	28.151
	[0, 1000]	≤ 0.002	20	15	0.9995	0.0005	394.371

Table 2: SMC results for temperature control

LTL formula	I (sec)	$\prec p$	$\alpha_{ch,1}$	T_{ZASP}	T_{CWSP}	Confidence	δ	time (sec)
$\diamond_I(P_{Ch,1} \geq 1)$	[0,500]	≥ 0.98	0.65	20	17	0.95	0.05	43.712
	[0,500]	≤ 0.02	0.65	25	20	0.95	0.05	38.65
	[0,500]	≤ 0.02	1	25	20	0.95	0.05	41.784
	[0,500]	≤ 0.02	1	25	20	0.995	0.005	71.627
	[0,500]	≤ 0.02	1	25	20	0.95	0.005	1025.492

Table 3: SMC results for cooling load.

LTL formula	I (sec)	Max kWh	confidence	δ	# runs	time (sec)	Pr
$\diamond_I(P_w \geq \text{Max})$	[0, 500]	1.5	0.95	0.05	738	53.185	[0,0.05]
	[0, 1000]	1.5	0.95	0.05	738	108.872	[0,0.0744]
	[0, 3000]	1.5	0.95	0.05	738	259.849	[0.338,0.438]
	[0, 3000]	2	0.95	0.05	738	258.456	[0.329,0.429]
	[0, 3000]	2.5	0.95	0.05	738	259.671	[0.314,0.414]
	[0, 3000]	2	0.995	0.05	1199	424.564	[0.316,0.416]
	[0, 3000]	2	0.95	0.005	73778	25824.784	[0.369,0.379]

Table 4: Maximum wind production.

LTL formula	$I(\text{sec})$	ST	WT	MT	confidence	δ	# runs	time (in s)	Pr
$\diamond_I(fr \leq -0.1)$	[10,1000]	No	2	No	0.95	0.05	738	320.793	[0.95,1]
	[10,1000]	No	4	No	0.95	0.05	738	320.582	[0.95,1]
	[10,1000]	No	2	Yes	0.95	0.05	738	306.094	[0,0.05]
	[10,1000]	Yes	2	Yes	0.995	0.05	1199	1215.123	[0,0.05]
$\diamond_I(fr \geq 0.4)$	[10,500]	No	2	No	0.95	0.05	738	330.797	[0.425,0.525]

Table 5: SMC results for microgrid operating in islander mode

automata. The main contribution is the simulation and analysis of the combined behaviour of all these components. We reported on various simulation experiments and statistical model checking a number of bounded LTL properties using UPPAAL-SMC. In our case study we were not confronted with *rare events* [13]. Our model is more extensive than the piecewise deterministic Markov process model recently reported in [22]; it copes with more general and more detailed dynamics, and includes thermal energy. This case study has shown that stochastic hybrid automata are an adequate modeling formalism for modeling microgrids in a faithful manner. Statistical model checking seems an effective technique to evaluate bounded temporal properties of interest. Substantial effort in the model checking process has been spent on adopting the formal models to the syntactic restrictions of the UPPAAL-SMC.

References

1. A. Abate, J.-P. Katoen, J. Lygeros & M. Prandini (2010): *Approximate Model Checking of Stochastic Hybrid Systems*. *European J. of Control* 16(6), pp. 1–18.
2. A. Abate, J.-P. Katoen & A. Mereacre (2011): *Quantitative automata model checking of autonomous stochastic hybrid systems*. In: *Hybrid Systems: Computation and Control (HSCC)*, ACM, pp. 83–92.
3. G. Anderson (2012): *Dynamics and Control of Electric Power Systems*. Lecture Notes, ETH Zurich.
4. Howard Barringer, Yliès Falcone, Bernd Finkbeiner, Klaus Havelund, Insup Lee, Gordon J. Pace, Grigore Rosu, Oleg Sokolsky & Nikolai Tillmann, editors (2010): *Runtime Verification - First International Conference, RV 2010, St. Julians, Malta, November 1-4, 2010. Proceedings. Lecture Notes in Computer Science* 6418, Springer. Available at <http://dx.doi.org/10.1007/978-3-642-16612-9>.
5. C. Carrillo, Obando Montao, J. Cidrs & E. Daz-Dorado (2013): *Review of power curve modelling for wind turbines*. *Renewable and Sustainable Energy Reviews* 21(0), pp. 572 – 581, doi:<http://dx.doi.org/10.1016/j.rser.2013.01.012>. Available at <http://www.sciencedirect.com/science/article/pii/S1364032113000439>.
6. C. Cassandras & J. Lygeros (2007): *Stochastic Hybrid Systems*. Taylor & Francis.
7. A. David, D. Du, K. G. Larsen, A. Legay, M. Mikucionis, D. Poulsen & S. Sedwards (2012): *Statistical Model Checking for Stochastic Hybrid Systems*. In: *Workshop on Hybrid Systems and Biology (HSB)*, EPTCS 92, pp. 122–136.
8. Nicolas Gensollen, Vincent Gauthier, Michel Marot & Monique Becker (2013): *Modeling and optimizing a distributed power network : A complex system approach of the prosumer management in the smart grid*. CoRR abs/1305.4096. Available at <http://arxiv.org/abs/1305.4096>.
9. J.M. Gordon & K.C. Ng (1995): *Predictive and diagnostic aspects of a universal thermodynamic model for chillers*. *Int. J. of Heat and Mass Transfer* 38(5), pp. 807–818, doi:[doi:10.1016/0017-9310\(94\)00208-D](https://doi.org/10.1016/0017-9310(94)00208-D).
10. Ernst Moritz Hahn, Arnd Hartmanns, Holger Hermanns & Joost-Pieter Katoen (2013): *A compositional modelling and analysis framework for stochastic hybrid systems*. *Formal Methods in System Design* 43(2), pp. 191–232. Available at <http://dx.doi.org/10.1007/s10703-012-0167-z>.
11. A. Hartmanns & H. Hermanns (2012): *Modelling and Decentralised Runtime Control of Self-stabilising Power Micro Grids*. In: *ISoLA (1)*, LNCS 7609, pp. 420–439.
12. A. Hartmanns, H. Hermanns & P. Berrang (2012): *A comparative analysis of decentralized power grid stabilization strategies*. In: *Winter Simulation Conference (WSC)*, WSC, pp. 1–13.
13. C. Jégourel, A. Legay & S. Sedwards (2012): *Cross-Entropy Optimisation of Importance Sampling Parameters for Statistical Model Checking*. In: *International Conference on Computer Aided Verification (CAV)*, LNCS 7358, pp. 327–342.
14. Young Joo Kim, Moonzoo Kim & Tai-Hyo Kim (2012): *Statistical Model Checking for Safety Critical Hybrid Systems: An Empirical Evaluation*. In: *Haifa Verification Conference (HVC)*, pp. 162–177.
15. R. Lasseter (2011): *Smart Distribution: Coupled Microgrids*. *Proceedings of the IEEE* 99(6), pp. 1074–1082. Available at <http://dx.doi.org/10.1109/JPROC.2011.2114630>.
16. J. Machowski, J.W. Bialek & J.R. Bumby (2008): *Power System Dynamics - Stability and Control*. John Wiley & Sons.
17. Knut W. Mathisen, Manfred Morari & Sigurd Skogestad (1994): *Dynamic models for heat exchangers and heat exchanger networks*. *Computers & Chemical Engineering* 18, Supplement 1(0), pp. S459 – S463, doi:[http://dx.doi.org/10.1016/0098-1354\(94\)80075-8](http://dx.doi.org/10.1016/0098-1354(94)80075-8). Available at <http://www.sciencedirect.com/science/article/pii/S0950423094000439>.
18. J. Mur-Amada & A.A. Bayod-Rujula (2007): *Wind Power Variability Model – Part II – Probabilistic Power Flow*. In: *9th Int. Conf. on Electrical Power Quality and Utilisation (EPQU 2007)*, pp. 1–6.
19. A. Parisio & L. Glielmo (2011): *Energy efficient management using Model Predictive Control*. In: *50th IEEE Conf. on Decision and Control and European Control Conference (CDC-ECC 2011)*, pp. 5449–5454. Available at <http://dx.doi.org/10.1109/CDC.2011.6161246>.
20. K. Philippopoulos & D. Deligiorgi (2009): *Statistical simulation of wind speed in Athens, Greece, based on Weibull and ARMA models*. *J. of Energy* Vol. 3, pp. 151–158.
21. F. Ramponi, D. Chatterjee, S. Summers & J. Lygeros (2010): *On the connections between PCTL and dynamic programming*. In: *Hybrid Systems: Computation and Control (HSCC)*, ACM, pp. 253–262.
22. M. Strelec, K. Macek & A. Abate (2012): *Modeling and Simulation of a Microgrid as a Stochastic Hybrid System*. In: *IEEE Conf. on Innovative Smart Grid Technologies (ISGT)*, IEEE, pp. 1–9.
23. M. Tigges (2010): *Modellbasierte Analyse zur Verbesserung der elektrischen Energiebereitstellung*.

- zu künftiger Offshore-Windparks mittels Biogastechnologie. Ph.D. thesis, Universitaet Paderborn.
24. J. Tzanos, K. Margellos & J. Lygeros (2011): *Optimal wind turbine placement via randomized optimization techniques*. In: *Power Systems Comput. Conf. (PSCC)*, pp. 1–8.
 25. H. Younes & R. G. Simmons (2006): *Statistical probabilistic model checking with a focus on time-bounded properties*. *Inf. Comput.* 204(9), pp. 1368–1409.
 26. S. Younes, E. M. Clarke, G. J. Gordon & J. G. Schneider (2005): *Verification and Planning for Stochastic Processes with Asynchronous Events*. Technical Report.